PCCP

Excess entropy scaling for the segmental and global dynamics of polyethylene melts

Journal:	*Physical Chemistry Chemical Physics*
Manuscript ID:	CP-ART-08-2014-003559.R1
Article Type:	Paper
Date Submitted by the Author:	17-Sep-2014

Complete List of Authors:	Voyiatzis, Evangelos; Technische Universität Darmstadt , Mueller-Plathe, Florian; Technische Universitat Darmstadt, Böhm, Michael; Technical University of Darmstadt,

Excess entropy scaling for the segmental and global dynamics of polyethylene melts

Evangelos Voyiatzis, Florian Müller-Plathe and Michael C. Böhm

Eduard-Zintl-Institut für Anorganische und Physikalische Chemie and Center of Smart Interfaces, Technische Universität Darmstadt, Alarich-Weiss-Strasse 4, D-64287Darmstadt, Germany

Dedicated to Prof. Dr. Karl Jug on the occasion of his 75th birthday

Abstract

The range of validity of the Rosenfeld and Dzugutov excess entropy scaling laws is analyzed for unentangled linear polyethylene chains. We consider two segmental dynamical quantities, i.e. the bond and the torsional relaxation times, and two global ones, i.e. the chain diffusion coefficient and the viscosity. The excess entropy is approximated by either a series expansion of the entropy in terms of the pair correlation function or by an equation of state for polymers developed in the context of the self associating fluid theory. For the whole range of temperatures and chain lengths considered, the two estimates of the excess entropy are linearly correlated. The scaled bond and torsional relaxation times fall into a master curve irrespective of the chain length and the employed scaling scheme. Both quantities depend non-linearly on the excess entropy. For a fixed chain length, the reduced diffusion coefficient and viscosity scale linearly with the excess entropy. An empirical reduction to a chain length-independent master curve is accessible for both dynamic

quantities. The Dzugutov scheme predicts an increased value of the scaled diffusion coefficient with increasing chain length which contrasts physical expectations. The origin of this trend can be traced back to the density dependence of the scaling factors. This finding has not been observed previously for Lennard-Jones chain systems (Macromolecules 46 (2013) 8710-8723). Thus, it limits the applicability of the Dzugutov approach to polymers. In connection with diffusion coefficients and viscosities, the Rosenfeld scaling law appears to be of higher quality than the Dzugutov approach. An empirical excess entropy scaling is also proposed which leads to a chain length-independent correlation. It is expected to be valid for polymers in the Rouse regime.

1. Introduction

The difficulties in the direct calculation of transport properties of soft matter systems have triggered the development of alternative techniques for their estimation. One route is based on establishing relations between dynamic properties, on the one hand, and structural or thermodynamic parameters, on the other [1-10]. Several phenomenological structural correlations on the basis of intuitively selected combinations of macroscopic quantities have been employed successfully in this context [2,3,11-13]. A possible way for correlating transport and structural properties is the adoption of the excess entropy as representative structural parameter. The excess entropy scaling law proposed by Rosenfeld [9,10] has been one of the first useful attempts which has inspired further developments in the field. The most prominent extensions are the Dzugutov [5] and the Bretonnet [7,8] excess entropy scaling laws.

Rosenfeld developed his scaling law on the basis of arguments that provide a macroscopic description of soft matter systems [9,10]. The derivation of the reduction parameters is based on the assumption that the characteristic length- and time-scales of

dynamic processes in simple monoatomic systems can be related i) to the mean interparticle distance l, $l = \rho^{-1/3}$ where ρ is the atomic number density, and ii) to the average thermal velocity of the atoms u_{th}, $u_{\mathrm{th}} = \sqrt{\mathrm{k_B T/m}}$ where $\mathrm{k_B}$ is the Boltzmann constant, T the temperature and m the atomic mass. With the help of theses quantities, we observe the following Rosenfeld (Ros) scaling for the diffusion coefficient, D, and viscosity, η: $\mathrm{D_{Ros}} = \mathrm{D}\rho^{1/3}/\sqrt{\mathrm{k_B T/m}}$ and $\eta_{\mathrm{Ros}} = \eta\rho^{-2/3}/\sqrt{\mathrm{mk_B T}}$. The final Rosenfeld entropy scaling expressions read $\mathrm{D_{Ros}} = 0.6\exp\left(0.8\mathrm{S_{ex}}\right)$ and $\eta_{\mathrm{Ros}} = 0.2\exp\left(-0.8\mathrm{S_{ex}}\right)$. The parameter $\mathrm{S_{ex}}$ is the excess entropy per atom normalized by the Boltzmann constant. Thus, it is dimensionless. Rosenfeld's scaling has gained much attention because it can be adapted easily for systems of experimental interest [14-20]; the reduction parameters depend on quantities whose estimation is simple and direct.

Dzugutov's (Dz) scaling constitutes an alternative excess entropy scaling formulation. Its derivation is based on two arguments; for short time-scales the momentum and energy transfer is dominated by short-range repulsive interparticle interactions which can be described approximately as collisions between hard spheres. It conveys the microscopic picture that each atom is "trapped" within a cage formed by its immediate neighbors. The characteristic time-scale of this process is the collision frequency of an atom with its surrounding cage, Γ_{E}, which is given by $\Gamma_{\mathrm{E}} = 4\mathrm{r_{max}^2 g_2}\left(\mathrm{r_{max}}\right)\rho\sqrt{\pi \mathrm{k_B T/m}}$. Here $\mathrm{r_{max}}$ is the distance at which the first maximum in the pair correlation function $\mathrm{g_2}$ appears, i.e. $\mathrm{g_2(r_{max})}$. For longer times, all dynamic processes are influenced by the relaxation rate of the cage; this rate is proportional to the number of accessible configurations per atom, i.e. to the exponential of the excess entropy. These considerations form the basis of the Dzugutov scaling which reads $\mathrm{D_{Dz}} = \mathrm{D}/(\mathrm{r_{max}^2}\Gamma_{\mathrm{E}}) = 0.049\exp(\mathrm{S_2})$. The parameter $\mathrm{S_2}$ is the pair entropy per atom normalized by the Boltzmann constant. In the original publication [5], the reduction parameters of the Dzugutov scaling have been derived for a hard sphere

system. The selection of an appropriate mapping scheme for fluids with both repulsive and attractive interactions onto an equivalent hard sphere description improves the quality and range of validity of this scaling law [21]. We see, that typical time-scales in the Dzugutov approach can be related to dynamic phenomena in polymer physics, such as reptation. When compared to Rosenfeld, the Dzugutov scaling employs only the pair excess entropy and not the total excess entropy of the system. Moreover, the reduction parameters characterize the microstructure of the system and not its overall macroscopic state. It has been shown [23,24] that the Dzugutov scaling is globally less accurate than that of Rosenfeld for short hard sphere and Lennard-Jones chains. The former scaling is only linear over a restricted range of the excess entropy around -2.5. In the case of hard sphere chains and alkanes, the Dzugutov scaling depends not only on excess entropy but also on a size parameter [24].

The Rosenfeld and Dzugutov excess entropy scalings have been proposed for simple monoatomic systems without internal architecture. In subsequent studies, the validity of the excess entropy scalings has been examined in a variety of physical systems of higher complexity which posses an intrinsic architecture such as liquid metals [14,22], ionic liquids [15], network-forming ionic melts [16], hydrocarbon isomer fluids [17], alkanes [24], colloidal monolayers [18], unentangled [23,24] as well as entangled [25] polymer model chains. The excess entropy scaling laws have been also extended to describe confined systems [19,20,26-29]. Due to the inherent difficulties in determining the excess entropy of such systems, possibilities to employ alternative quantities, such as the heat capacity [30] or the effective packing density [27], have been investigated. The effective packing density is defined as the product of the particle number density and the third power of the equivalent hard sphere diameter of the particles. Quite generally, however, these scalings are of lower accuracy than the excess entropy schemes [27,30].

The adoption of excess entropy scaling laws as a practical tool to predict transport properties has been hindered by the following reasons. i) They are empirical phenomenological laws lacking a sound theoretical foundation. The rationalization of a well defined theoretical background has been the topic of several studies since their introduction [31-33]. ii) Furthermore, they have been developed for single component systems and their extension to multicomponent samples is not always trivial. The description of multicomponent systems leads to a challenge when scaling the mutual diffusion coefficient [34]. Nevertheless, there have been several efforts to extend the applicability of the above scalings to multicomponent systems [34-37]. iii) Finally, excess entropy scaling laws are valid only when the scaled transport properties are single-valued functions of the excess entropy. Otherwise two different states of a given system with the same excess entropy but different dynamic properties cannot be described unambiguously. The breakdown of excess entropy scalings in systems with thermodynamic anomalies, i.e. the observation of a diffusion coefficient increasing with increasing density or pressure, has been discussed critically [38,39]. Recent advances in the formulation of the excess entropy scaling laws and the selection of the scaling factors in the context of both the Rosenfeld and Dzugutov theories have overcome this hurdle [40-42].

The present work explores the range of validity of excess entropy scalings for both global and segmental dynamic properties of polyethylene (PE) using molecular dynamics (MD) simulations. Four unentangled chain lengths (n) are considered; their molecular weights are 352, 702, 1402 and 2102 g/mol corresponding to n = 25, 50, 100 and 150 carbon atoms. The PE entanglement length has been determined as 156 carbon atoms corresponding to a molecular weight of 2186 g/mol [43]. We investigate the scaling of both global dynamic properties, such as the viscosity and the diffusion coefficient, as well as of segmental ones, such as the bond and torsional relaxation times. The two most widely accepted scaling schemes are employed, i.e. the Rosenfeld and the Dzugutov methods. The

excess entropy is approximated using either conformational data or an equation of state (EoS) derived in the context of the self associating fluid theory (SAFT) [44,45]. Although the parameters of the SAFT EoS are not directly related to the employed force field, the latter scheme provides a computationally inexpensive and uncomplicated way of approximating the entire excess entropy of the system taking into account all possible contributions. Alternative methods such as thermodynamic integration are much more sophisticated and demanding. The correlation between the two entropy estimates is investigated. The present study extends the discussion of previous works on excess entropy scalings of idealized Lennard-Jones chains [23,25] and hydrocarbon isomer fluids [17] to a real unentangled polymer with a simple monomer architecture.

2. Systems and computational methods

The systems under investigation are monodisperse. They contain 100 linear PE chains. Their chain and entanglement lengths have been given above. Each system is studied at five different temperatures: T = 400, 425, 450, 475 or 500 K. The pressure is 101.325 kPa. The PE chains are represented as linear strings of united atoms where only the carbon atoms are considered explicitly [46]. A flexible bond version [47] of a specially developed PE force field [46] is employed. A detailed description can be found elsewhere [46,47]. A spherical cut-off distance of 1.2 nm and long-range corrections for the potential energy and the pressure are used [48].

The initial configurations are created using a simplified “bond growth” procedure with an initial density of 0.75 g/cm^3. The only imposed restriction is that the distance between any nonbonded pair of united atoms should exceed 0.395 nm. The configurations are subjected to energy minimization using the Polak-Ribière version of the conjugate gradient method [49]. The systems are equilibrated by means of Monte Carlo simulations

[46]. Long MD calculations are carried out in the canonical (NVT) ensemble. The equations of motion are integrated using the velocity Verlet algorithm. A time step of 1 fs is used. The Nosè Hoover thermostat [48] is employed and the systems are further relaxed for 10 ns. The production runs are also performed in the NVT ensemble. The simulation time required for the calculation of the diffusion coefficient is 150 ns. All computations are performed using the LAMMPS code [50].

The normalized bond autocorrelation function (ACF), P_B, is defined as

$$P_B(t) = \left\langle \hat{\mathbf{b}}_{ij}(t) \cdot \hat{\mathbf{b}}_{ij}(0) \right\rangle \quad (1)$$

where $\langle \ldots \rangle$ denotes an ensemble average, $\hat{\mathbf{b}}_{ij}(t)$ the normalized bond vector between the i^{th} and the j^{th} united atoms at time t. The normalized bond ACF is fitted to a modified Kohlrausch–Williams–Watts (mKWW) function $f(t)$. It is defined by a fast decaying exponential with a prefactor a to describe the librational moves of the bond vectors and a slow KWW function associated with the segmental motion of the polymer:

$$f(t) = a \exp(-t/b) + (1-a) \exp\left(-[t/c]^d\right) \quad (2)$$

The area under $f(t)$ defines the bond relaxation time $\tau_B = \int_0^\infty f(t)dt$. The relaxation time of the mKWW function can be derived analytically; i.e. $\tau_B = a\,b + (1-a)\,c\,\Gamma(d^{-1})/d$, where Γ is the gamma function [51]. The torsional autocorrelation function, P_ϕ, reads

$$P_\phi(t) = \frac{\left\langle \cos(\phi(t))\cos(\phi(0)) \right\rangle - \left\langle \cos(\phi(0)) \right\rangle^2}{\left\langle \cos(\phi(0))\cos(\phi(0)) \right\rangle - \left\langle \cos(\phi(0)) \right\rangle^2} \quad (3)$$

where the torsional angle ϕ is defined by four consecutive united atom carbons. Similarly to the case of the normalized bond ACF, the mKWW expression allows an adequate description of the time evolution of P_ϕ. The torsional relaxation time, τ_t, is also obtained by analytical integration of the mKWW function. It agrees in its structure with τ_B.

The diffusion coefficient of the centre of mass (COM) of the chains, D_{COM}, is calculated using the Einstein formalism

$$D_{COM} = \lim_{t\to\infty} \frac{1}{6t} \left\langle \left[\mathbf{r}_{COM,i}(t) - \mathbf{r}_{COM,i}(0) \right]^2 \right\rangle \quad (4)$$

where $\mathbf{r}_{COM,i}(t)$ is the position vector of the COM of the i^{th} chain at time t. The viscosity, η, is computed by mapping the atomistic trajectories to the Rouse model [43]. This method predicts that the viscosity of an unentangled system is inversely related to the diffusion coefficient according to

$$\eta = \frac{\rho_n R_{Gas} T \left\langle R_{ee}^2 \right\rangle}{36 D_{COM}} \quad (5)$$

where ρ_n is the chain number density of the system, R_{Gas} the universal gas constant and R_{ee} the end-to-end distance vector of the chains. The validity of our approach has been already confirmed by Harmandaris et al. [43] where the crossover from the Rouse to the entangled polymer melt regime has been studied.

3. Entropy estimation

The direct calculation of the excess entropy of a molecular system is prohibited due to the absence of a suitable averaging formalism. Thus, several methods have been developed to overcome this problem [52-54]. The next paragraphs provide a description of two of these methods to calculate the excess entropy: either by an entropy series expansion in terms of many-body correlation functions or by an EoS based on SAFT.

3.1 Configurational route

Intuitively, it is expected that the entropy of a molecular system, S, and its internal structure, especially its conformational properties, are tightly interconnected. A formal proof on the grounds of statistical mechanics has been given [55], thus justifying a series expansion of the entropy in terms of many-body correlations of the system. It reads $S = S_{id} + \sum_{i=2}^{\infty} S_i$ where S_{id} is the entropy per atom of an "ideal gas" ensemble at the same thermodynamic conditions as the system under consideration and S_i is the atomically normalized entropy due to correlations involving a number of i atoms. The excess entropy per atom of the system, S_{ex}, is defined as the difference between S and its "ideal gas" contribution, S_{id}: $S_{ex} = S - S_{id} = \sum_{i=2}^{\infty} S_i$.

The simplest approximation to estimate S_{ex} is to take into account only the pair entropy, S_2, while neglecting all higher order elements. The most dominant contribution to S_2 is the translational part [25]. In this case the excess entropy of the system can be written as

$$S_{ex} \cong S_2 = -2\pi\rho\int_0^{\infty}\left(g_2(r)\ln\left(g_2(r)\right) - g_2(r) + 1\right)r^2 dr \qquad (6)$$

where r is the distance measured relative to a chosen united atom reference carbon. The pair correlation function includes all intramolecular and intermolecular pairs but excludes the contribution from the bonded first neighbors of each united atom [23,25]. A significant advantage of this route is that the entropy can be computed easily with small statistical uncertainties compared to other methods [48]. The influence of the temperature on the structure of the pair correlation function $g_2(r)$ is shown in Fig. 1 for a PE chain with 150 carbon atoms. The system is studied at three different temperatures: T = 400, 450 and 500 K. The positions of the maxima and the minima of $g_2(r)$ are located at roughly the same interparticle distances r for all temperatures studied. Higher peaks and deeper valleys are formed with decreasing temperature. In additional simulations, we have found that chain

length variations have an almost negligible influence on the pair correlation function (see Fig. S1 in Supporting Information). An increase of the chain length under constant temperature leads to a slightly higher first peak, which should be attributed to the increased density and cohesiveness of the system.

The variation of the pair entropy S_2 (per atom) with the temperature of the system and chain length is shown in Fig. 2a. The observed negative S_2 values are expected as the reference state is that of an "ideal gas" of united atoms which is characterized by complete randomness and a lack of any kind of correlations. The employed force field reduces the number of accessible configurations relative to the ones in the reference state of an "ideal gas". The computed S_2 values can be correlated accurately with the temperature and the chain length of the system. The empirical formula $S_2 = -10.2\left(1 - 0.126\ln(T)\right)(1 - 4.27/n)$ is valid for all cases under consideration. The small mean square error of $3.3\ 10^{-4}$ shows that a factorization of S_2 in terms of $\ln(T)$ and $1/n$ is possible. An increase in the temperature and a decrease of the chain length lead both to larger absolute values of the pair entropy. For an infinitely long PE chain ($n \to \infty$), the system reaches a hypothetical asymptotic entropy value which depends only on temperature; it reads $S_{2,n\to\infty} = -10.2\left(1 - 0.126\ln(T)\right)$. Note that this extrapolation is based on unentangled PE chains, a condition which is not valid in infinitely long real systems. The same restriction has to be considered in connection with the asymptotic curve in Fig. 2b which has been derived within the SAFT framework. The continuous line in Fig. 2a corresponds to such an asymptotic entropy value for an infinitely long chain as predicted by our empirical formula for S_2. A similar factorization of S_2 as indicated above in terms of $\ln(T)$, ρ and $1/n$ has been also found for Lennard-Jones chain systems [25]. It reads $S_2 = -3.188\left(1 - 0.205\ln(T_{LJ})\right)\left(1 - 0.374/\rho_{LJ}\right)(1 + 0.091/n)$ where T_{LJ} and ρ_{LJ} are the temperature and number density of the system in reduced Lennard-Jones units. The differences in the numerical values of the

coefficients of these two entropy correlations reflect the differences in the employed force fields and the simulation conditions (temperature range and pressure). We have found a stronger chain length dependence in the PE case than in the Lennard-Jones one.

3.2 Perturbed Chain Self Associating Fluid Theory

An alternative route to the calculation of the excess entropy is to employ an EoS which reproduces the thermodynamic properties of the system of interest. We have chosen the Perturbed Chain (denoted as PC) SAFT EoS as it has been applied successfully to several polymer systems [44,45,56,57]. An advantage of this approach over the configurational route is that an estimate of the total excess entropy is obtained which takes into account all possible entropy contributions due to many-body correlations. Nevertheless, the PC SAFT EoS has several parameters, which in almost all cases have been optimized against experimental data. Although, in principle, such data sets can be obtained from molecular simulations, this task is computationally very demanding. As a matter of fact such an approach has been rarely employed. Despite recent advances [58,59], it is still not possible to parametrize directly the PC SAFT EoS on the basis of interaction parameters of an atomistic force field. Thus, an internal consistency between the SAFT excess entropy and the adopted force field is not guaranteed.

The PC SAFT EoS is not formulated in terms of the excess entropy of a system but attempts to model the excess Helmholtz free energy, $\mathrm{A_{ex}}$. The excess entropy is then obtained by temperature differentiation of the excess Helmholtz free energy. For monodisperse PE systems, $\mathrm{A_{ex}}$ is written as the sum of a hard chain reference contribution, $\mathrm{A_{ex,hc}}$, and a dispersion contribution, $\mathrm{A_{ex,disp}}$ leading to $\mathrm{A_{ex}} = \mathrm{A_{ex,hc}} + \mathrm{A_{ex,disp}}$ [44,45]. The first term describes the excluded volume effects in the system. The second attractive term is

treated as a perturbation of the reference system. A complete description of the PC SAFT EoS and its elements can be found elsewhere [44,45]. PC SAFT EoS has been successful in predicting the vapour-liquid equilibrium and the liquid density of pure polyethylene melts over a wide range of thermodynamic conditions as well as the solubility of small ethylene molecules in polyethylene melts [45]. The parameters for both low density and high density PE have been tested [44]; the differences in the calculated entropies are negligible.

The variation of the SAFT based excess entropy, S_{SAFT}, with the temperature and the chain length is shown in Fig. 2b. Increasing chain lengths lead to larger negative S_{SAFT} values. For the two shorter systems, we find that the estimated excess entropy depends strongly on the chain length. When the systems approach the entangled regime, S_{SAFT} reaches a limiting n independent curve. Such a saturation is also observed for S_2, as predicted by the empirical factorization of S_2 in terms of $1/n$ and $\ln(T)$. A similar scaling of S_{SAFT} with $1/n$ has been identified in a previous study for short unentangled Lennard-Jones chains [23]. A comparison of the excess entropy estimates for PE and Lennard-Jones chains under the same thermodynamic conditions and chain lengths has revealed considerable differences in their actual values. The S_{SAFT} values for PE are 50 % up to 100 % larger than the corresponding S_{SAFT} ones for Lennard-Jones chains. The differences between the two estimates are enlarged with increasing chain length. This discrepancy should be attributed to the less flexible structure of a PE chain relative to a Lennard-Jones chain with the same length. The decreased flexibility is caused by the adoption of angle-bending and torsional potentials in the PE force field.

The correlation of S_{SAFT} with S_2 is presented in Fig. 3. In the same figure, we have also incorporated S_{SAFT} - S_2 data for short unentangled Lennard-Jones chains which are available in the literature [23]. They are shown by a continuous blue line. This correlation intends to quantify the influence of two different employed models on the excess entropy.

The PE data form a master curve for all chain lengths and temperatures considered. A linear correlation of the form $S_{SAFT} = 1.82 + 1.88S_2$ with $R^2 = 0.99$ is valid for the entire entropy domain in our study. The values of S_{SAFT} closest to zero (i.e. right hand side of Fig. 3) are less negative than those of S_2. In this entropy region, S_2 predicts a less "disordered" state than S_{SAFT}. This observation is in contrast with the *a priori* expectation that S_{SAFT} should be larger in magnitude than S_2. Remember that the former entropy estimation takes into account all possible many-body interactions while the latter neglects all entropy contributions that are higher than of the pair type. The observed entropy grading should be attributed to the parametrization procedure of the PC SAFT EoS. Its elements have been obtained for much longer systems than the ones at hand. In contrast to linear Lennard-Jones chains, a fragmentation of the entropy domain into two regimes is not necessary. We assume that this improved correlation between the two entropy estimates can be explained by the fact that the PC SAFT EoS takes into account correlations beyond the intramolecular bond ones [23,25] while Lennard-Jones SAFT EoS neglects any information of intramolecular ordering beyond the bond distribution. When comparing the data of the PE systems with the ones of the Lennard-Jones chains, we observe smaller differences between S_2 and S_{SAFT} in the PE case. Given that the adoption of angle and torsional potentials increases the stiffness of a molecule and restricts the motion of the atoms, this behavior is an indication of an increased contribution of the pair entropy to the overall excess entropy. We also notice that the slope of the entropy correlation in the PE systems is steeper than the one in the Lennard-Jones chains cases.

4. Dynamic properties

The concept of "strongly correlated fluids" [60,61] provides a theoretical framework to justify the existence of several phenomenological laws in molecular systems such as the

excess entropy scaling law. A fluid is classified as “strongly correlated” when the fluctuations of the potential energy from its thermodynamic average are well correlated to the fluctuations of the virial. The corresponding correlation coefficient should be greater than 0.9. The variation of this correlation coefficient with respect to the temperature for various chain lengths is shown in Fig. 4. The observed correlation is rather weak and the correlation coefficient ranges between 0.61 and 0.65, i.e. it is too small to justify the label “strongly correlated”. Both an increase of the chain length or a temperature decrease cause slightly higher correlation coefficients.

4.1 Scaling of segmental relaxation times

In the subsequent sections we discuss the scaling behavior of segmental and global dynamical properties with the two adopted excess entropy estimators. All dynamic quantities of interest are made dimensionless according to either the Rosenfeld or the Dzugutov scaling laws. The scaling behavior of the bond and the torsional relaxation times is presented first, followed by an analysis of the entropy scaling of the diffusion coefficient and viscosity.

Our starting point is the examination of excess entropy scalings of two segmental dynamic properties: the bond, τ_B, and torsional, τ_T, relaxation times. Both the Rosenfeld and the Dzugutov theories provide a characteristic short time-scale which may serve as normalization factor in such cases. In the context of the Dzugutov scaling, the segmental relaxation time can be made dimensionless by the inverse of the collision frequency Γ_E. The normalization factor based on the Rosenfeld scaling is defined as the ratio of the mean interparticle distance l and the mean thermal velocity of the particles u_{th}. Both τ_B and τ_T are expected to depend only weakly on the chain length [46,47].

The correlation of the Rosenfeld or Dzugutov scaled bond relaxation times, $\tau_{B,Ros}$ and $\tau_{B,Dz}$, with S_{SAFT} as well as S_2 is presented in Fig. 5. Irrespective of the employed scaling scheme and the way the excess entropy is estimated, the data can be approximated by a single master curve for all chain lengths and temperatures considered. The Dzugutov and Rosenfeld theories postulate that any normalized dynamic property should scale linearly with an exponential of the excess entropy [5,9,10]. In contrast to this expectation, the master curves in Fig. 5 show a nonlinear behavior. Guided by similar findings in previous studies, where the segmental dynamics of hydrocarbon isomer fluids [17] and water [62] have been studied, we have fitted the data by the series expansions given in Table 1. For the $\tau_{B,Ros}$ - S_2 case, an attempt to fit the data to a linear expression has been also made. The resulting expression reads $\ln(\tau_{B,Ros}) = -6.09 - 4.77S_2$ with $R^2 = 0.86$. Both fitting curves are presented in Fig. S2 in the Supporting Information where the limitations of a linear fit are illustrated. Similar trends are observed for the remaining three cases. The observed scattering of the data in the S_2 case is slightly smaller than in S_{SAFT} . The regression coefficient R^2 for the Rosenfeld scaling amounts to $R^2 = 0.91$ when S_{SAFT} is adopted and to $R^2 = 0.93$ for the S_2 approximation. This splitting seems to be caused by the fact that S_2 is extracted from the simulation data while S_{SAFT} is not linked to them. The difference between the two R^2 values is however too small to allow an unambiguous explanation.

Additionally, we have analyzed the relation between the Rosenfeld or the Dzugutov scaled torsional relaxation time, $\tau_{T,Ros}$ and $\tau_{T,Dz}$, and both excess entropy estimates. These correlations are shown in Fig. 6. A similar behavior as already discussed for the scaled bond relaxation time is observed. Also the data of Fig. 6 can be mapped by nonlinear master curves. The expressions providing accurate fits are given in Table 2 together with the regression coefficients. We observe that the scaled τ_T vary in a much smaller range than the scaled τ_B. When the coefficients of the present PE excess entropy scalings are compared

with the coefficients of similar expressions for hydrocarbon isomer fluids [17], we can conclude that such correlations are system specific; they are not transferable to materials with a different chemistry.

4.2 Diffusion coefficient scaling

An important molecular transport property is the diffusion coefficient, D_{COM}. Both the Dzugutov and Rosenfeld excess entropy scalings have been developed initially for simple systems such as monoatomic fluids [5,9,10]. Their application to molecular systems with a more complex architecture requires a simple modification of the scaling parameters. A molecular version of the Rosenfeld scaling is obtained when the atomic number density, ρ, and the atomic mass, m, are replaced by the chain number density, ρ_n, and the mass of a polymeric chain, m_n. The reduced Rosenfeld diffusion coefficient, $D_{COM,Ros}$, reads $D_{COM,Ros} = D_{COM}\rho_n^{1/3} \Big/ \sqrt{k_B T / m_n}$.

The original Dzugutov scaling has also been adapted to take into account the molecular characteristics of the entire polymeric chain. The reduced Dzugutov diffusion coefficient reads $D_{COM,Dz} = D_{COM} \Big/ \left(r_{max}^2 \Gamma_{E,n} \right)$ where the collision frequency is equal to $\Gamma_{E,n} = 4 r_{max}^2 g_2 \left(r_{max} \right) \rho_n \sqrt{\pi k_B T / m_n}$. In the following, we will test the usefulness of linear correlations of the form $\ln\left(D_{COM,Scaled}\right) = A(n) + \alpha(n) S_{ex}$ for both scalings (Ros, Dz).

The variation of the two scaled diffusion coefficients, $D_{COM,Ros}$ and $D_{COM,Dz}$ with the entropy estimates S_{SAFT} and S_2 is presented in Fig. 7. As anticipated, we have found that D_{COM} is reduced with increasing chain length following the scaling predicted by the Rouse theory [43]. The Rouse theory is based on the physical picture of an unentangled polymer chain reptating along the contour of a tube which is dictated by the presence of the

surrounding chains. Given that the excess entropy becomes more negative with increasing chain length (see Fig. 3), it is expected that the scaled values of the diffusion coefficient are also reduced with decreasing values of the excess entropy. Such a trend has been observed in Lennard-Jones chain systems for both the Rosenfeld and the Dzugutov schemes [23,25]. For the studied PE chains this is only valid for $D_{COM,Ros}$. In contrast to this behavior, $D_{COM,Dz}$ becomes larger when the chain length is increased. Although this connection between $D_{COM,Dz}$ and the excess entropy seems to be unphysical, it does not prevent the applicability of the Dzugutov scheme for excess entropy correlations in polymers.

For a given chain length, a linear dependence of the natural logarithm between the scaled diffusion coefficient and the excess entropy is observed. The scaling parameters in each case can be related to the chain length; the resulting expressions are given in Table 3. For infinitely long chains, a limiting value for all parameters can be derived. The limitations of such an extrapolation have been emphasized already in connection with Fig. 2, i.e. the neglect of entanglements. A dependence of the scaling parameters on $1/n$ has been detected. The same functional dependence of the scaling parameters on $1/n$ in long Lennard-Jones chains has been observed previously [25]. Nevertheless, it differs from the behavior for short unentangled ones [23] where a weaker $\sqrt{1/n}$ dependence of the scaling parameters has been identified. In the Dzugutov scheme, we observe that the system with the shortest chains, i.e. n = 25, differs from the other chains. A closer inspection of the Dzugutov scaling factors reveals that this deviation should be attributed to the chain density dependence of $\Gamma_{E,n}$. Both r_{max} and $g(r_{max})$ have an almost constant value which depends very weakly on the temperature and the chain length (see Fig. 1 and Fig. S1 in Supporting Information). Our simulations confirm previous findings that the mass density and the chain density depend nonlinearly on n [46]. This dependence induces stronger ρ_n variations as a function of n for shorter PE chains than for longer ones [63]. The Rosenfeld scaling employs

a non-integral power (less than one) of the chain density, i.e. $\rho_n^{1/3}$, which prevents observing an increased value of the scaled diffusion coefficient with larger in absolute magnitude excess entropy values. Such a trend between the scaled diffusion coefficient and the excess entropy has not been observed previously in studies of Lennard-Jones chains [23,25]. The empirical correlations given in Table 3 imply that the coefficients α_{Ros} and α_{Dz} increase with increasing n. Since we employ the excess entropy per molecular segment (i.e. per carbon atom) rather than per molecule (i.e. for the whole PE chain), we assume that the increased values of α_{Ros} and α_{Dz} with increasing chain length are a manifestation of increasing intramolecular contributions to the excess entropy.

The elements A_{Ros} and A_{Dz} in the correlations for the diffusion coefficient depend on n in all cases considered. This finding is in line with previous studies for Lennard-Jones chains [23,25] as well as hard sphere chains and alkanes [24]. Let us come back to the correlation $\ln(D_{COM,Scaled}) = A(n) + \alpha(n)S_{ex}$. When correlating $\ln(D_{COM,Scaled}) - A(n)$ directly with the two excess entropy estimates, a single master curve for all chain lengths is found; see Fig. S3 in the Supporting Information. This allows the interpretation of $A(n)$ as a hypothetical limiting diffusion coefficient when the excess entropy of the system is zero. Note that the statement is only valid in the absence of phase transitions.

A major difference between the present study and two previous ones [23,25], which have dealt with chain molecules, refers to the conditions under which the simulations have been performed. The temperature range considered in the manuscript at hand varies from 8.7 up to 10.9 in Lennard-Jones units while the maximum value in the previous studies [23,25] has been 5.0. Similarly, the adopted scaled number density ranges between 1.71 and 2.08 while the maximum value considered previously has been 0.9 [23,25]. Nevertheless, we have attempted a comparison between a recent [23] and the present work. The variation of the scaled Rosenfeld diffusion coefficient with S_{SAFT} for PE and Lennard-Jones chains is

shown in Fig. 8. The data for the Lennard-Jones chains have been obtained from the respective correlation given in Goel et al. [23]. Although the two excess entropy scalings share the same qualitative features, the actual values in the Lennard-Jones case depend stronger on the chain length. This behaviour is caused by the differences in the chemical nature of the two systems. It might be that a better agreement between the two excess entropy scalings can be found if the Lennard-Jones and PE systems are mapped by equivalent freely jointed chains.

The two scalings considered so far lead to correlations with chain length dependent parameters. To avoid this dependence, we have attempted to develop an empirical scaling leading to correlations with parameters depending only on the architecture and the chemistry of the polymer. For this purpose, we have adopted the characteristic length-scale r_{max} of the Dzugutov scaling and the characteristic time-scale of the atomic version of the Rosenfeld scaling. Guided by the Rouse theory, which predicts that the diffusion coefficient is inversely proportional to the number of Kuhn segments of the polymer chain, we have also included the factor n/c_n in our scaling, where c_n is the characteristic ratio of the polymer chain. The final reduced diffusion coefficient reads $D_{COM,F} = D_{COM}\left(n/c_n\right)\Big/\left(r_{max}\sqrt{k_B T/m}\right)$. The variation of the $D_{COM,F}$ with the SAFT entropy estimate S_{SAFT} is shown in Fig. 9. We observe that the two longest PE systems fall into the same linear master curve while a satisfactory agreement is also noted for the system with 50 carbons per chain. The data have been fitted to the equation $\ln\left(D_{COM,F}\right) = 1.698 S_{SAFT} - 0.058$ with a regression coefficient $R^2 = 0.92$. We expect that the developed scaling will be applicable to polymers which are in the Rouse regime. The employed parameters should depend only on the architecture and chemistry of the chain.

4.3 Viscosity scaling

For the present problem, the reduction parameters of the original Rosenfeld scaling have been adjusted in a way that they describe chain instead of atomic properties. The molecular version of the Rosenfeld viscosity scaling is $\eta_{Ros} = \eta\rho_n^{-2/3} \Big/ \sqrt{m_n k_B T}$. Similarly, a molecular version of the Dzugutov viscosity scaling has been developed [14]. The scaled Dzugutov viscosity, η_{Dz}, for a molecular system reads $\eta_{Dz} = \eta r_{max} \Big/ \left(\Gamma_{E,n} m_n \right)$. It should be noted that the viscosity has been determined by employing the Rouse model as expressed by Eq. (5). This means that the viscosity is related to the inverse of the diffusion coefficient of the PE chains and, thus, no pronounced differences in the accuracy for the viscosity and the diffusion coefficient as well as for their scaling behavior are expected. We have confirmed the validity of our approach to compute the viscosity by performing independent calculations for the shortest PE system using the Green - Kubo stress relation. The obtained viscosity values were characterized by higher statistical uncertainties than those based on the Rouse model while the observed differences between them were always less than 10 %. Thus, the results from the two approaches are in good agreement; differences are rather small.

The variation of the scaled viscosity with S_{SAFT} and S_2 is shown in Fig. 10. The observed scattering is similar to the one encountered in the case of the diffusion coefficient. In the present work, we focus on the development of a linear correlation which reads $\ln(\eta_{Scaled}) = B(n) + \beta(n) S_{ex}$ for a given chain length. It is possible to correlate the coefficients of each scaling quantitatively with the inverse of the chain length. These correlations are given in Table 4 for both scaling schemes. A limiting value for the scaling parameters is reached for very long PE chains. In analogy to the Dzugutov scaled diffusion coefficient, a differing behavior of η_{Dz} is again observed for the shortest chain length which should be attributed to variations of the chain density with increasing chain lengths.

5. Conclusions

The present simulation study has explored whether dynamic properties of a real polymer scale with its excess entropy. Four unentangled PE systems over a wide range of temperatures have been considered in our approach. We have studied both segmental dynamic properties, such as the bond and the torsional relaxation times, and global ones, such as the viscosity and the diffusion coefficient. The excess entropy is approximated either by employing the PC SAFT EoS or by using a series expansion of the excess entropy in terms of the pair correlation function.

We compared the predictions of the two ways to approximate the excess entropy. Despite the fact that the parameters of the SAFT EoS are not directly linked to the employed force field and that SAFT has been parameterized against experimental data describing the thermodynamic properties of considerably longer chains, a simple linear correlation between the two estimates is valid for all chain lengths and temperatures considered. For all dynamic properties considered, both excess entropy approximations lead to scalings of almost the same quality which share the same characteristic features. Therefore, in consideration of their linear correlation, they appear to be equivalent for the case of unentangled polyethylene chains.

The scaling of the segmental dynamics leads always to a master curve, irrespective of the scaling scheme and the way the excess entropy is approximated. Contrary to the original theories, the scaled segmental dynamics does not depend linearly on the excess entropy. We have established correlations which are valid for the entire entropy domains. The coefficients of these correlations do not dependent on the chain length. Both scaling laws provide expressions of the same quality.

The diffusion coefficient and the viscosity scale linearly with the excess entropy when the chain length is fixed. The scaling parameters correlate well with the inverse of the chain length. The applicability of the Dzugutov scheme to PE samples is limited when analyzing the scaled diffusion coefficient. It predicts the rather unphysical result that the scaled parameter increases with increasing chain length. The quality of the excess entropy scaling is improved when employing the Rosenfeld instead of the Dzugutov scheme as well as S_2 instead of S_{SAFT}. We have also developed and tested the applicability of a set of reduction parameters which provides a chain length-independent excess entropy scaling. We expect that this scheme is valid for short unentangled linear polymer chains in the melt state, i.e. in the Rouse regime. In the case of the diffusion coefficient and the viscosity, the Rosenfeld scheme works better than the Dzugutov method in the limit of short chains which exhibit a stronger density dependence as a function of the chain length.

Acknowledgments

The present work has been supported by the EU project Nanomodel (No. 211778) and the Deutsche Forschungsgemeinschaft by the Priority Program 1369 Polymer-Solid Contacts: Interfaces and Interphases.

References

1. F. Llovell, R.M. Marcos and L.F. Vega, *J. Phys. Chem. B*, 2013, **117**, 8159–8171

2. D. Fragiadakis and C.M. Roland, *J. Chem. Phys.*, 2011, **134**, 044504-1 - 044504-3

3. E.R. Lopez, A.S. Pensado, M.J.P. Comunas, A.A.H. Padua, J. Fernandez and K.R. Harris, *J. Chem. Phys.*, 2011, **134**, 144507-1 - 144507-11

4. A. Allal, C. Boned and A. Baylaucq, *Phys. Rev. E*, 2001, **64**, 011203-1 - 011203-10

5. M. Dzugutov, *Nature*, 1996, **381**, 137 – 139

6. S.E. Quiñones-Cisneros and U.K. Deiters, *J. Phys. Chem. B*, 2006, **110**, 12820 – 12834

7. J.L. Bretonnet, *J. Chem. Phys.*, 2002, **117**, 9370 - 9373

8. J.L. Bretonnet, *J. Chem. Phys.*, 2004, **120**, 11100 - 11106

9. Y. Rosenfeld, *Phys. Rev. A*, 1977, **15**, 2545 - 2549

10. Y. Rosenfeld, *Chem. Phys. Lett.*, 1977, **48**, 467-468

11. E.R. López, A.S. Pensado, J. Fernández and K.R. Harris, *J. Chem. Phys.*, 2012, **136**, 214502-1 - 214502-7

12. K. Satoh, *J. Chem. Phys.*, 2013, **139**, 084901-1 - 084901-11

13. A. Grzybowski, K. Grzybowska, M. Paluch, A. Swiety and K. Koperwas, *Phys. Rev. E*, 2011, **83**, 041505-1 - 041505-7

14. G.X. Li, C.S. Liu and Z.G. Zhu, *J. Non-Cryst. Sol.*, 2005, **351**, 946 – 950

15. M. Malvaldi and C. Chiappe, *J. Chem. Phys.*, 2012, **132**, 244502-1 - 244502-6

16. M. Agarwal, M. Singh, B.S. Jabes and C. Chakravarty, *J. Chem. Phys.*, 2011, **134**, 014502-1 - 014502-7

17. R. Chopra, T.M. Truskett and J.R. Errington, *J. Phys. Chem. B*, 2010, **114**, 16487–16493

18. X. Ma, W. Chen, Z. Wang, Y. Peng, Y. Han and P. Tong, *Phys. Rev. Lett.*, 2013, **110**, 078302-1 - 078302-5

19. B.J. Borah, P.K. Maiti, C. Chakravarty, and S. Yashonath, *J. Chem. Phys.*, 2012, **136**, 174510-1 - 174510-8

20. P. He, H. Liu, J. Zhu, Y. Li, S. Huang, P. Wang and H. Tian, *Chem. Phys. Lett.*, 2012, **535**, 84-90

21. F.W. Starr, S. Sastry, J.F. Douglas and S.C. Glotzer, *Phys. Rev. Lett.*, 2002, **89**, 125501-1 - 125501-4

22. A.K. Metya, A. Hens and J.K. Singh, *Fluid Phase Equilibria*, 2012, **313**, 16–24

23. T. Goel, C.N. Patra, T. Mukherjee and C. Chakravarty, *J. Chem. Phys.*, 2008, **129**, 164904-1 - 164904-9

24. R.V. Vaz, A.L. Magalhães, D.L.A. Fernandes and C.M. Silva, *Chem. Eng. Sc.*, 2012, **79**, 153-162

25. E. Voyiatzis, F. Müller-Plathe and M.C. Böhm, *Macromolecules*, 2013, **46**, 8710-8723

26. J. Mittal, J.R. Errington and T.M. Truskett, *Phys. Rev. Lett.*, 2006, **96**, 177804-1 - 177804-4

27. J. Mittal, J.R. Errington and T.M. Truskett, *J. Phys. Chem. B*, 2007, **111**, 10054–10063

28. W.P. Krekelberg, D.W. Siderius, V.K. Shen, T.M. Truskett and J.R. Errington, *Langmuir*, 2013, **29**, 14527–14535

29. P. He, H. Li and X. Hou, *Chem. Phys. Lett.*, 2013, **593**, 83 - 88

30. T.S. Ingebrigtsen, J.R. Errington, T.M. Truskett and J.C. Dyre, *Phys. Rev. Lett.*, 2013, **111**, 235901-1 - 235901-6

31. C. Kaur, U. Harbola and S.P. Das, *J. Chem. Phys.*, 2005, **123**, 034501-1 - 034501-6

32. S.P. Das, *Phys. Rev. E*, 1996, **54**, 1715-1719

33. U. Harbola, C. Kaur and S.P. Das, *Phys. Rev. Lett.*, 2003, **91**, 229601-1 - 229601-1

34. A. Samanta, A.S. Musharaf and S.K. Ghosh, *Phys. Rev. Lett.*, 2001, **87**, 245901-1 - 245901-4

35. W. Krekelberg, M.J. Pond, G. Goel, V.K. Shen, J.R. Errington and T.M. Truskett, *Phys. Rev. E*, 2009, **80**, 061205-1 - 061205-13

36. S. Musharaf Ali, A. Samanta, N. Choudhury and S.K. Ghosh, *Phys. Rev. E*, 2006, **74**, 051201-1 - 051201-6

37. A. Samanta, S. Musharaf Ali and S.K. Ghosh, *J. Chem. Phys.*, 2005, **123**, 084505-1 - 084505-5

38. Y.D. Fomin, V.N. Ryzhov and N.V. Gribova, *Phys. Rev. E*, 2010, **81**, 061201-1 - 061201-12

39. Y.D. Fomin, E.N. Tsiok and V.N. Ryzhov, *J. Chem. Phys.*, 2011, **135**, 124512-1 - 124512-13

40. M. Agarwal, M. Singh, R. Sharma, M. Parvez Alam and C. Chakravarty, *J. Phys. Chem. B*, 2010, **114**, 6995–7001

41. E. Salcedo, A. Barros de Oliveira, N.M. Barraz Jr., C. Chakravarty and M.C. Barbosa, *J. Chem. Phys.*, 2011, **135**, 044517-1 - 044517-9

42. M. Agarwal, M. Parvez Alam and C. Chakravarty, *J. Phys. Chem. B*, 2011, **115**, 6935–6945

43. V.A. Harmandaris, V.G. Mavrantzas, D.N. Theodorou, M. Kröger, J. Ramirez, H.C. Ottinger and D. Vlassopoulos, *Macromolecules*, 2003, **36**, 1376-1387

44. J. Gross and G. Sadowski, *Ind. Eng. Chem. Res.*, 2002, **41**, 1084-1093

45. J. Gross and G. Sadowski, *Ind. Eng. Chem. Res.*, 2001, **40**, 1244-1260

46. N.C. Karayiannis, V.G. Mavrantzas and D.N. Theodorou, *Phys. Rev. Lett.*, 2002, **88**, 105503-1 - 105503-4

47. G. Tsolou, N. Stratikis, C. Baig, P.S. Stephanou and V.G. Mavrantzas, *Macromolecules*, 2010, **43**, 10692-10713

48. D.S. Frenkel and B. Smit, *Understanding Molecular Simulation. From Algorithms to Applications*; Academic Press, California, USA, **2001**

49. J.E.S. Dennis and R.B. Schnabel, *Numerical Methods for Unconstrained Optimization and Nonlinear Equations*; SIAM Press, Philadelphia, USA, **1987**

50. S. Plimpton, *J. Comp. Phys.*, 1995, **117**, 1-19

51. M. Abramowitz and I.A. Stegun, *Handbook of Mathematical Functions with Formulas, Graphs, and Mathematical Tables*; Dover Publications, New York, USA, **1972**

52. F. Wang and D.P. Landau, *Phys. Rev. Lett.*, 2001, **86**, 2050 - 2053

53. M.S. Shell, P.G. Debenedetti and A.Z. Panagiotopoulos, *Phys. Rev. E.*, 2002, **66**, 056703-1 - 056703-9

54. R. Sharma, M. Agarwal and C. Chakravartya, *Mol. Phys.*, 2008, **106**, 1925-1938

55. A. Baranyai and D.J. Evans, *Phys. Rev. A*, 1989, **40**, 3817 - 3822

56. I.A. Kouskoumvekaki, N. von Solms, T. Lindvig, M.L. Michelsen and G.M. Kontogeorgis, *Ind. Eng. Chem. Res.*, 2004, **43**, 2830–2838

57. A. Tihic, G.M. Kontogeorgis, N. von Solms, M.L. Michelsen and L. Constantinou, *Ind. Eng. Chem. Res.*, 2008, **47**, 5092–5101

58. C. Avendaño, T. Lafitte, C.S. Adjiman, A. Galindo, E.A. Müller and G. Jackson, *J. Phys. Chem. B*, 2013, **117**, 2717–2733

59. C. Avendaño, T. Lafitte, A. Galindo, C.S. Adjiman, G. Jackson and E.A. Müller, *J. Phys. Chem. B*, 2011, **115**, 11154-11169

60. N.S. Gnan, T.B. Schrøder, U.R. Pedersen, N.P. Bailey and J.C. Dyre, *J. Chem. Phys.*, 2009, **131**, 234505-1 - 234505-17

61. T.S.S. Ingebrigtsen, T.B. Schrøder and J.C. Dyre, *Phys. Rev. X*, 2012, **2**, 011011-1 - 011011-20

62. R. Chopra, T.M. Truskett and J.R. Errington, *J. Phys. Chem. B*, 2010, **114**, 10558 - 10566

63. L.J. Fetters, D.J. Lohse, D. Richter, T.A. Witten and A. Zirkel, *Macromolecules*, 1994, **27**, 4639–4647

Table 1: Rosenfeld and Dzugutov excess entropy scaling correlations and regression coefficients R^2 for the reduced bond relaxation time.

Rosenfeld scaling	Dzugutov scaling
$\ln(\tau_{B,Ros})$ = -9.726 -10.21S_{SAFT} -1.735S_{SAFT}^2 R^2=0.91	$\ln(\tau_{B,Dz})$ = -7.068 -10.44S_{SAFT} -1.733S_{SAFT}^2 R^2=0.93
$\ln(\tau_{B,Ros})$ = -40.10 -36.39S_2 -7.305S_2^2 R^2=0.93	$\ln(\tau_{B,Dz})$ = -38.26 -37.17S_2-7.386S_2^2 R^2 = 0.94

Table 2: Rosenfeld and Dzugutov excess entropy scaling correlations and regression coefficients R^2 for the reduced torsional relaxation time.

Rosenfeld scaling	Dzugutov scaling
$\ln(\tau_{T,Ros}) = 5.236 - 0.717S_{SAFT}-0.058S_{SAFT}^2$ R^2=0.93	$\ln(\tau_{T,Dz})$ = 7.955 -0.837S_{SAFT} -0.017S_{SAFT}^2 R^2=0.92
$\ln(\tau_{T,Ros})$ = 2.768 -2.634S_2 -0.410S_2^2 R^2 = 0.94	$\ln(\tau_{T,Dz})$ = 4.629 -3.305S_2 -0.435S_2^2 R^2=0.93

Table 3: Rosenfeld and Dzugutov excess entropy scaling parameters for the reduced diffusion coefficient $\ln(D_{COM,Ros}) = A_{Ros} + \alpha_{Ros}S_{ex}$ and $\ln(D_{COM,Dz}) = A_{Dz} + \alpha_{Dz}S_{ex}$.

	A_{Ros}	α_{Ros}	A_{Dz}	α_{Dz}
$S_{ex,SAFT}$	0.083 / n - 2.861	-11.14 / n + 1.221	-110.4 / n + 1.247	-34.56 / n + 1.867
S_2	19.05 / n- 1.776	-15.51 / n + 2.182	-154.0 / n + 4.328	-54.87 / n + 3.337

Table 4: Rosenfeld and Dzugutov excess entropy scaling parameters for the reduced viscosity $\ln(\eta_{Ros}) = B_{Ros} + \beta_{Ros}S_{ex}$ and $\ln(\eta_{Dz}) = B_{Dz} + \beta_{Dz}S_{ex}$.

	B_{Ros}	β_{Ros}	B_{Dz}	β_{Dz}
$S_{ex,SAFT}$	-79.01 / n + 0.908	-12.42 / n - 1.595	-88.37 / n + 0.366	-11.97 / n - 1.434
S_2	-121.6 / n - 1.261	-38.28 / n - 2.818	-137.8 / n - 1.954	-35.85 / n - 2.544

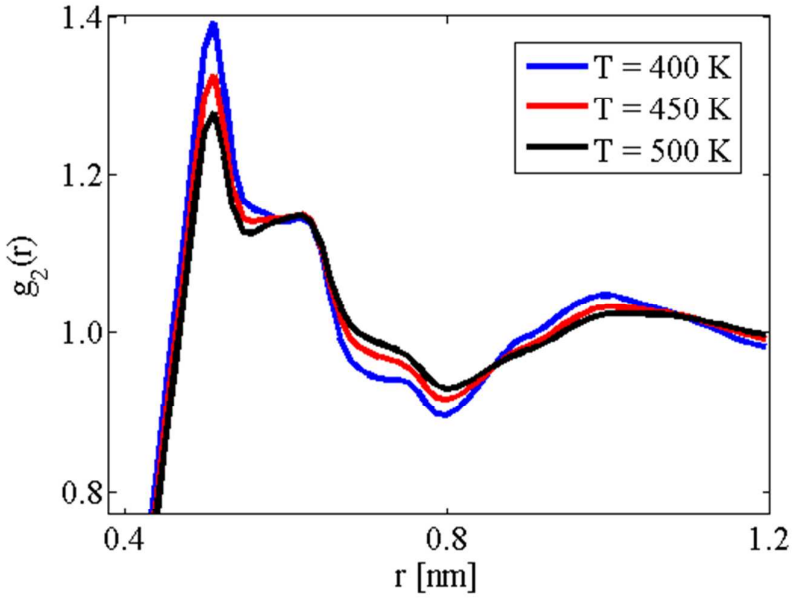

Figure 1. Structure of the pair correlation function $g_2(r)$ of a polyethylene chain with 150 carbon atoms as a function of the distance r measured relative to a chosen reference carbon atom. First neighbors on the same chain are excluded. $g_2(r)$ is presented for three different temperatures at a pressure of 101.325 kPa.

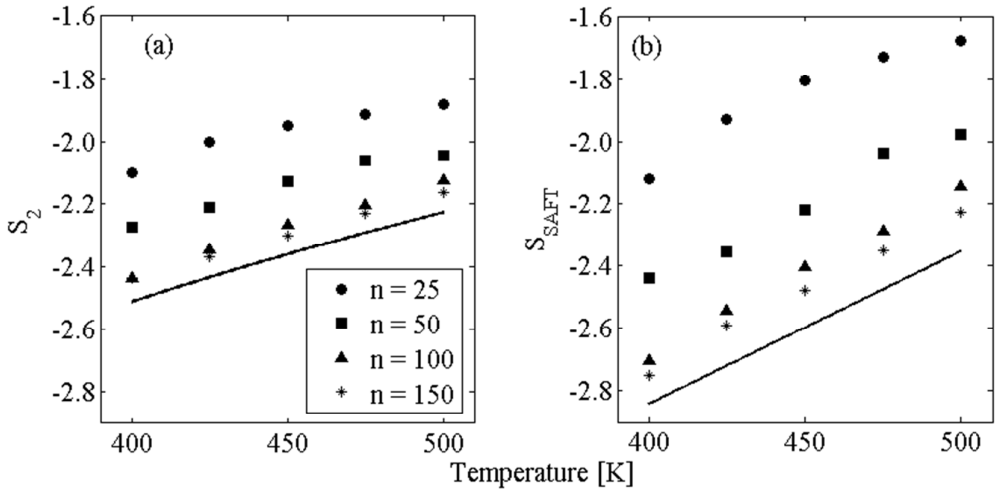

Figure 2. Temperature and chain length dependence of the pair entropy S_2 (part a) and the excess entropy based on SAFT, S_{SAFT}, (part b). Temperatures between 400 K and 500 K and chain lengths between 25 and 150 carbon atoms have been considered. The pressure of the systems has been fixed to 101.325 kPa. The full line in both diagrams refers to the asymptotic entropies for an infinitely long polyethylene chain.

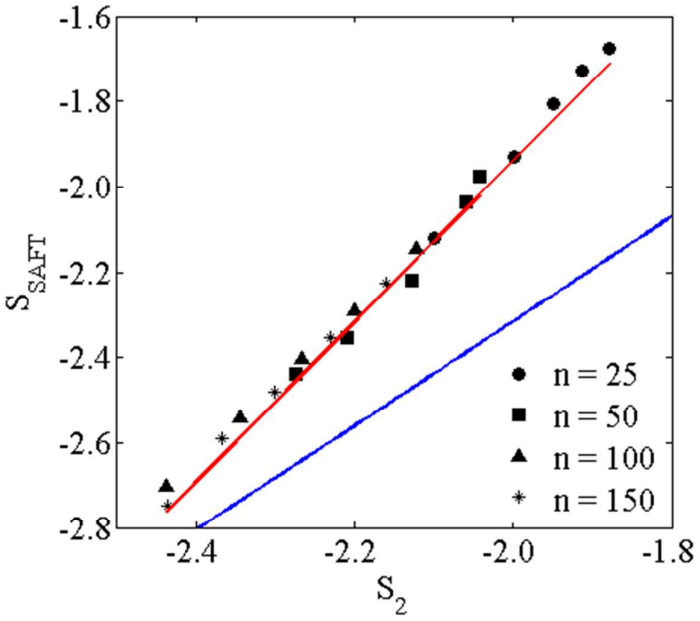

Figure 3. Correlation of the SAFT excess entropy, S_{SAFT}, with the pair entropy, S_2, for chain lengths between 25 and 150 carbon atoms. Temperatures between 400 K and 500 K have been considered. The continuous red line refers to the best linear fit between S_2 and S_{SAFT} for the polyethylene systems while the continuous blue line to the best linear fit obtained by Goel et al. [23] for unentangled Lennard-Jones chains.

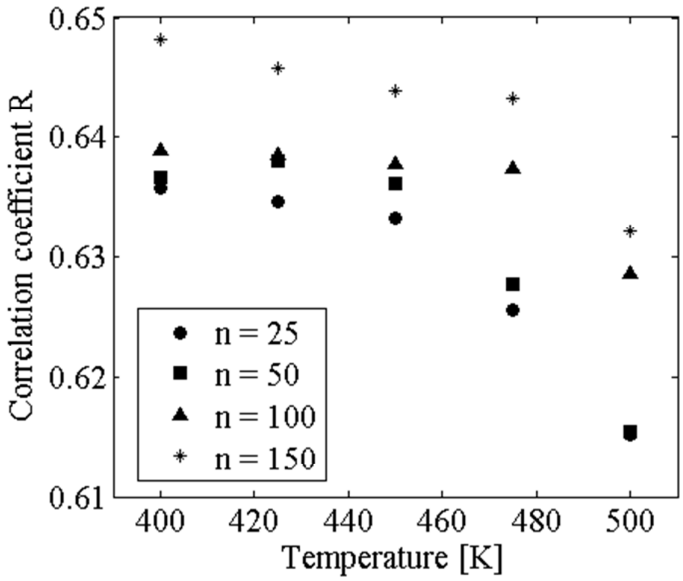

Figure 4. Correlation coefficient between the fluctuations of the virial and the fluctuations of the potential energy as a function of temperature for various chain lengths.

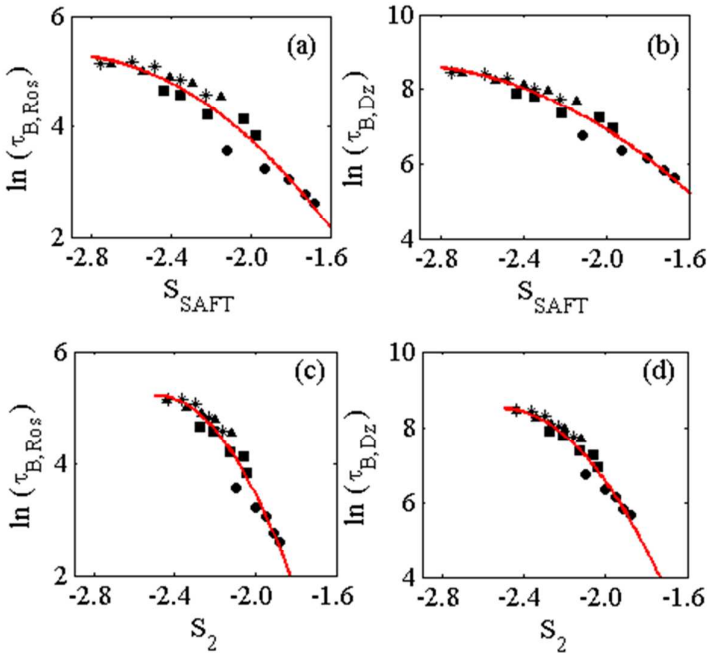

Figure 5. Correlation between the natural logarithm of both the Rosenfeld and the Dzugutov scaled bond relaxation time and the excess entropy, approximated either by SAFT, S_{SAFT}, or the pair entropy, S_2. We have adopted the same chain length symbols as adopted in Figs. 2 to 4. The red continuous lines correspond to the quadratic fits given in Table 1.

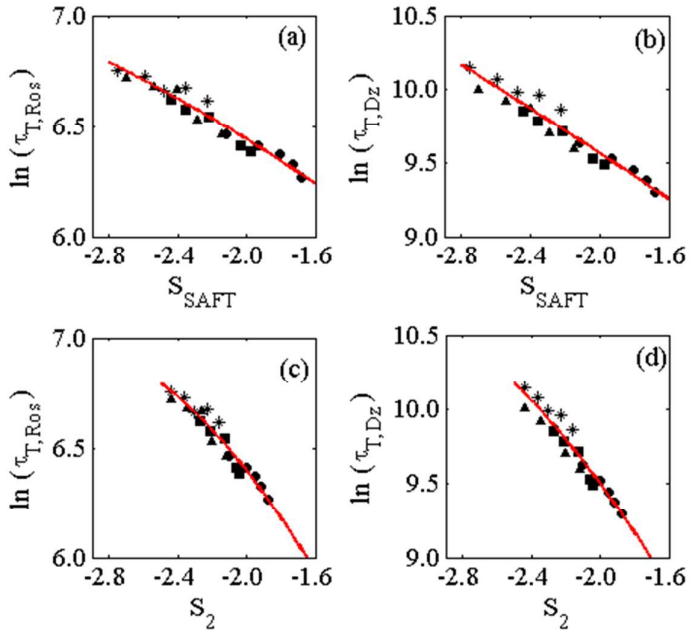

Figure 6. Variation of both the Rosenfeld and the Dzugutov scaled torsional relaxation time with the excess entropy, approximated either by SAFT or the pair entropy. The temperatures and chain lengths chosen correspond to the same setup as employed in the other correlation schemes. The red continuous lines correspond to the quadratic fits given in Table 2.

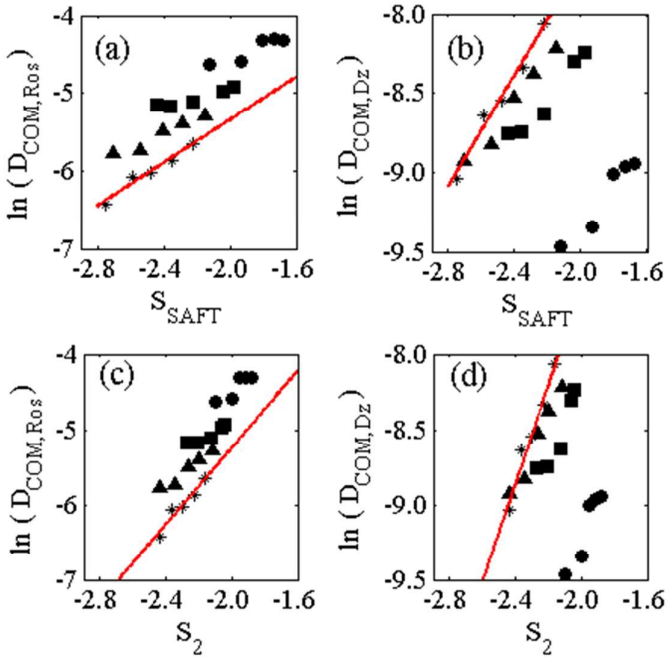

Figure 7. Variation of both the Rosenfeld and the Dzugutov scaled diffusion coefficient with the excess entropy, approximated either by SAFT or the pair entropy. The temperatures and chain lengths chosen correspond to the same setup as employed in the other correlation schemes. The red continuous lines correspond to the linear fits given in Table 3 for a chain length of 150 carbon atoms.

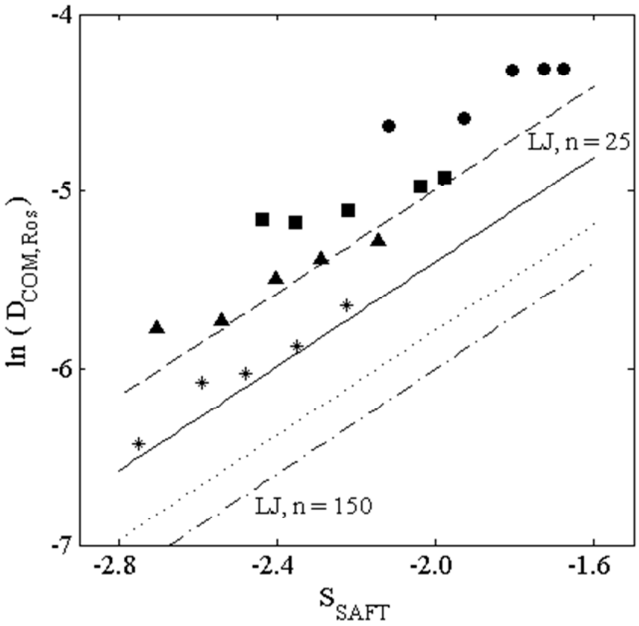

Figure 8. Variation of the scaled Rosenfeld diffusion coefficient with the SAFT excess entropy for PE and Lennard-Jones chains. The temperatures and chain lengths chosen correspond to the same setup as employed in the other correlation schemes. The lines represent the data

for the Lennard-Jones chains as considered in Goel et al. [23]. The length of the Lennard-Jones chains increases from top to bottom of the plot.

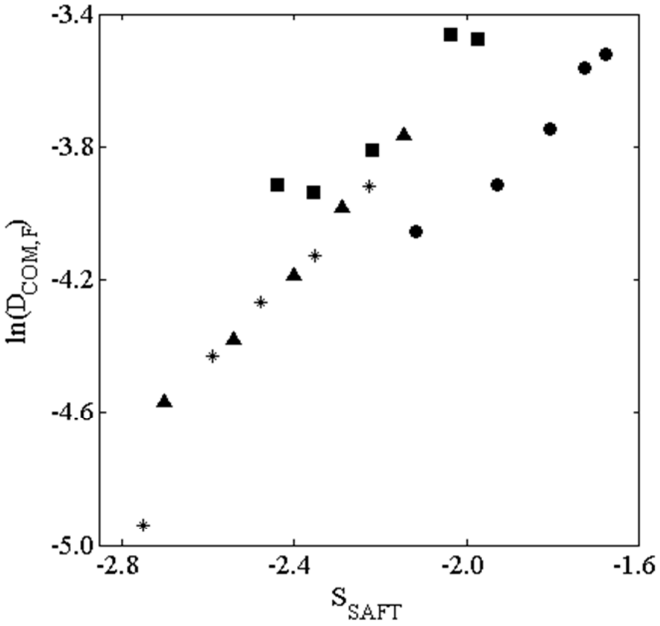

Figure 9. Variation of the proposed scaled diffusion coefficient with the SAFT excess entropy. The temperatures and chain lengths chosen correspond to the same setup as employed in the other correlation schemes.

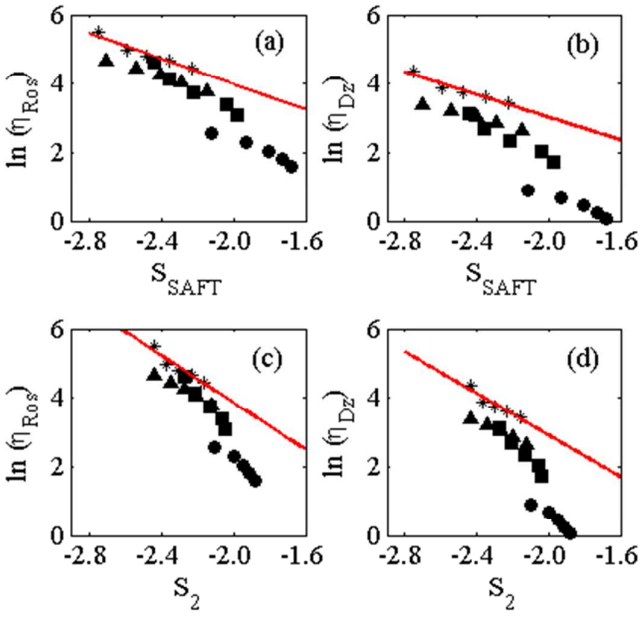

Figure 10. Variation of both the Rosenfeld and the Dzugutov scaled viscosity with the excess entropy, approximated either by SAFT or the pair entropy. The temperatures and chain lengths chosen correspond to the same setup as employed in the other correlation schemes. The red continuous lines correspond to the linear fits given in Table 3 for a chain length of 150 carbon atoms.